

Letter

GRACE—Gravity Data for Understanding the Deep Earth's Interior

Mioara Mandea ^{1,*}, Véronique Dehant ² and Anny Cazenave ³

¹ CNES—Centre National d'Études Spatiales, 75039 Paris, France

² Royal Observatory of Belgium, 1180 Brussels, Belgium; veronique.dehant@oma.be

³ LEGOS—Laboratoire d'Études en Géophysique et Océanographie Spatiales, Observatoire Midi-Pyrénées, 31400 Toulouse, France; anny.cazenave@legos.obs-mip.fr

* Correspondence: mioara.mandea@cnes.fr; Tel.: +33-6-76-28-17-85

Received: 12 November 2020; Accepted: 17 December 2020; Published: 21 December 2020



Abstract: While the main causes of the temporal gravity variations observed by the Gravity Recovery and Climate Experiment (GRACE) space mission result from water mass redistributions occurring at the surface of the Earth in response to climatic and anthropogenic forces (e.g., changes in land hydrology, ocean mass, and mass of glaciers and ice sheets), solid Earth's mass redistributions were also recorded by these observations. This is the case, in particular, for the glacial isostatic adjustment (GIA) or the viscous response of the mantle to the last deglaciation. However, it has only recently been shown that the gravity data also contain the signature of flows inside the outer core and their effects on the core–mantle boundary (CMB). Detecting deep Earth's processes in GRACE observations offers an exciting opportunity to provide additional insight into the dynamics of the core–mantle interface. Here, we present one aspect of the GRACEFUL (GRavimetry, mAgnetism and CorE Flow) project, i.e., the possibility to use gravity field data for understanding the dynamic processes inside the fluid core and core–mantle boundary of the Earth, beside that offered by the geomagnetic field variations.

Keywords: GRACE satellite; gravity field; magnetic field; core–mantle boundary

1. Introduction

Understanding the flow in the Earth's liquid outer core and its interactions with the lower mantle, as well as its effects on global Earth's observables such as the length-of-day (LoD) and gravity and magnetic fields, is an important topic. In order to estimate core flows, a knowledge of the core magnetic field and its temporal variations at the core–mantle boundary (CMB) [1,2] is needed together with a specific hypothesis about the flows. Core flows is a fundamental property of Earth's internal dynamics, but remain relatively poorly constrained. To address this topic, a multidisciplinary approach is needed. In a recently granted project by the European Research Council (ERC), called GRACEFUL (GRavimetry, mAgnetism and CorE Flow), we propose an integrative approach based on observations of the Earth's magnetic and gravity fields and LoD. In this special issue dedicated to Gravity Recovery and Climate Experiment (GRACE) missions, we focus mainly on how different factors that cause temporal variations of the gravity field (including atmospheric loading, land hydrology, land ice loss, and ocean mass change) can be estimated in order to obtain a residual signal that can be interpreted as the deep Earth's signature and that can be correlated with geomagnetic field variations. The approach is mainly data-driven, using data mostly provided by space missions.

With the advent of the space era about 50 years ago, determining the orbit of artificial satellites has become an imperative. Satellite orbits deform in a complex way over a broad range of timescales, mostly in response to the Earth's gravity field. Celestial mechanics theory together with “tracking” measurements between the ground geodetic stations and satellites have been used to determine the

satellite orbits from which models of the Earth's gravity have been derived. This has revealed that the gravity field is much more complex than previously thought, reflecting the heterogeneous distribution of the matter inside, at the surface, and above the surface of the planet. For many decades, however, only the "static" (i.e., time invariable) part of the gravity field has been measurable, except for the temporal change of the very low degree harmonics of the spherical harmonics expansion of the field [3–5]. The situation drastically improved in 2002 with the launch of the GRACE mission [6,7]. For the first time, GRACE provided gravity field solutions with global coverage, allowing the measurement of temporal changes of the Earth's gravity with unprecedented spatiotemporal resolution and precision.

The "static" Earth's gravity field represents the present heterogeneous distribution of the matter inside the Earth and on its surface. One of the gravity field equipotential surfaces forms the geoid, an equipotential surface that approximates the mean sea level at rest. Since the early 1970s, observations provided by artificial satellites have revealed that the geoid shape is much less regular than previously thought. Interpretation of the long wavelength undulations combined with seismic measurements of internal density variations has led to major advances in our understanding of the large-scale convective structure of the Earth's mantle, e.g., [8]. The next major step came in the early 2000s, with the ability to detect temporal changes of the gravity field, a real challenge since the static gravity field represents 99% of the total gravity signal. With a temporal resolution of ~1 month and a spatial resolution of ~300 km, GRACE-based gravity variations mostly reflect spatiotemporal variations of mass distributions occurring among the surface fluid envelopes of the Earth (atmosphere, oceans, terrestrial waters, and cryosphere) in response to climate change and variability (both from natural and anthropogenic sources) and to direct human interventions [7]. New data continue to be added to the GRACE record since the launch of the GRACE Follow-On (FO) mission in 2018.

GRACE and GRACE FO also measure solid Earth's processes such as co-seismic and post-seismic crustal deformations, e.g., [9,10], as well as large-scale readjustment of the Earth's mantle to the last deglaciation (the so-called glacial isostatic adjustment—GIA), e.g., [11]. GRACE also has the capability of detecting lithospheric deformations and associated gravity changes due to ongoing climate-related land ice melt [12,13]. While hundreds of scientific articles have been published during the past few years on the GRACE-based superficial mass redistributions, mass redistributions occurring deeper in the Earth have been the object of only a few investigations [1,2]. These studies also motivated the GRACEFUL project. Here, we propose to revisit the possibility to detect deep Earth's signals in the GRACE data using updated datasets over those in [1]. This paper needs to be seen as a short contribution to furthering the possibility of using space gravity data to gain better knowledge of core dynamics. We first briefly discuss magnetic field observations (Section 1) and show that the deep interior contribution in gravity field (Section 2) may be correlated with the geomagnetic field (Section 3). In the last section (Section 4), we discuss future prospects.

2. Materials and Methods

2.1. Magnetic Field Data Analysis

The study of the Earth's deep interior is in a period of significant evolution. The accumulation of seismic data provides important information on the material and physical properties of the core; however, only indirect observations are available on the dynamics of the Earth's fluid iron-rich outer core. Apart from seismic waves, the magnetic and gravity fields as well as the Earth's rotation provide invaluable information on processes occurring in the Earth's deep interior.

The geomagnetic field measured above the Earth's surface by different satellites or by magnetic observatories results from sources that are both internal and external to the planet. Dynamo action in the liquid outer core and crustal magnetization in the upper layers of the Earth constitute the internal sources, whereas electrical current systems in the ionosphere and magnetosphere are the external sources. The external ionospheric current systems are very complex in nature and appearance and vary rapidly with location and time. In the region in which satellite measurements are usually

taken (CHAMP, <https://isdc.gfz-potsdam.de/champ-isdc/>, and Swarm, <https://earth.esa.int/web/guest/swarm/data-access>), satellites fly between altitudes of roughly 300 and 500 km), and one important layer is the E-region, where electric currents flow on the dayside, in the altitude range of 90 to 150 km. Unless applying dedicated processing, the contributions from this region would be interpreted as internal sources by a satellite. It is thus crucial to understand the spatiotemporal scales associated with the contributions to the magnetic field from all the different sources.

The best possible models for the non-core sources must be used in order to extract the core field signal from satellite magnetic field measurements. Traditionally, the magnetic field is assumed to be measured in a source free region, thereby allowing for a description in terms of a potential field. This potential is typically expressed in terms of a spherical harmonics expansion. Two recent magnetic field models, GRIMM [14] and CHAOS [15], are worth considering. However, as shown in Figure 1, significant differences at the level of 10 nT between both fields can be seen in the polar areas, indicating an insufficient parametrization of the external field contributions in these regions. The leakage of external magnetic field signatures into the internal magnetic field model coefficients produces large-scale patterns. The cause for this leakage may be different data selection methods applied in the model derivations.

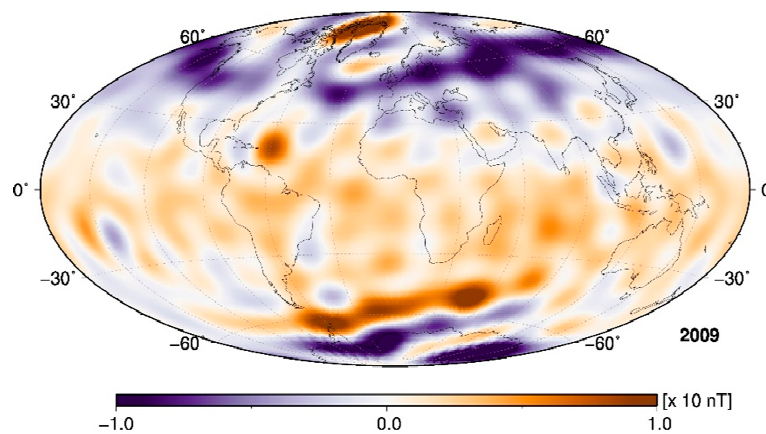


Figure 1. Differences of the radial magnetic core field at the Earth's surface derived from GRIMM [14] and CHAOS-6 [15].

To choose a magnetic field model or to compute such a model using magnetic observatories and satellite data is a very challenging task. It is imperative to focus on a rigorous separation of external and internal geomagnetic field sources and their individual temporal characteristics, in particular from intra-annual to inter-annual periods, as well as their noises in the same way as [16,17]. In the following, we consider the CHAOS-6 model, which describes the core magnetic field and its temporal variations, the secular variation, and secular acceleration [15].

2.2. Gravity Field Data Analysis

We analyzed monthly time series of GRACE gravity fields over the period January 2003 to December 2015 and extracted the deep solid Earth's signal, which is supposed to be correlated to the core magnetic field, after correcting for other well-known processes causing regional gravity variations. The latter include atmospheric loading, hydrological changes in river basins on land, glacier and ice sheet mass changes, ocean mass changes due to land ice melt and ocean circulation changes, and GIA [18].

To extract the time-variable deep Earth's signal from the GRACE data, we used the most up-to-date knowledge about each contribution (from the atmosphere, oceans, ice sheets and glaciers, terrestrial waters, etc.) and removed the corresponding signal from the GRACE fields over their

geographical areas of interest. We detail below the various datasets that we used as well as the methodology that we adopted to remove various components.

2.2.1. GRACE Fields

We used the ensemble mean of GRACE gravity field dataset processed by [19] (ftp://legos.obs-mip.fr/pub/soa/gravimetrie/grace_legos), available publicly (<ftp://legos.obs-mip.fr/pub/soa/gravimetrie/gracelegos>). This dataset consists of an average of five different GRACE solutions. They are based on spherical harmonics solutions provided by five different processing centers: the Center for Space Research at Texas University (CSR), GeoForschungsZentrum (GFZ), the Jet Propulsion Laboratory (JPL), the Technical University of Graz (TUG), and Groupe de Recherche de Géodésie Spatiale (GRGS). The “Release 5” solutions were used for the CSR, GFZ, and JPL datasets. “Release ITSG 2016” and “Release 3.3” were used for the TUG and GRGS solutions, respectively. For all GRACE solutions, the spherical harmonic coefficients up to degree 60 were used for the conversion to gridded mass anomalies. The post-processing applied by [19] includes: (i) the addition of independent estimates of the geocenter motion and Earth’s oblateness, as these quantities are either not or poorly observed by GRACE; (ii) a filtering for correlated errors characterized by north–south stripes; and (iii) a correction for the GIA. Different solutions have been considered in [19] for the geocenter, C_{20} , and GIA corrections in order to assess the GRACE data uncertainties. Here, we considered the gridded version of the ensemble mean of the five available solutions with the geocenter motion correction [20], C_{20} correction [21], and GIA model [22]. The GRACE data cover the time span of January 2003 to December 2015.

2.2.2. Atmospheric Loading and Associated Ocean Bottom Pressure

Atmospheric loading and associated ocean bottom pressure effects on GRACE solutions are accounted for by the processing centers using a priori background ocean and atmospheric models. However, different model corrections are used in the GRACE solutions considered here (hence the ensemble mean). To cope with this, in Reference [19] these models are added back to each GRACE solution, so that our own ocean and atmosphere background models can be used, and the same model for all solutions can be removed (see details in [19]). Atmospheric loading is removed in all available GRACE solutions, using atmospheric pressure fields from re-analyses of the European Center for Meteorological Weather Forecast (ECMWF).

2.2.3. Hydrological Component

The signature of terrestrial waters is the dominant signal in GRACE data over land, in addition to ice mass change of glaciers. Terrestrial waters include surface waters (rivers, lakes, wetlands, and man-made reservoirs), canopies, soil moisture, underground waters, and snowpack. Mass variations of these components are mainly driven by climate change and variability as well as human activities such as water extraction in aquifers for crop irrigation and domestic use, and reservoir construction at rivers. Multi-decadal trends of continental water mass are dominated by decreases due to groundwater depletion and by increases due to the construction of new reservoirs. Inter-annual variations are mainly driven by natural climate variability. Associated terrestrial water storage changes are routinely estimated from GRACE, e.g., [23–25]. However, to remove surface mass variations from GRACE data for further extraction of the deep Earth’s signal, independent data are needed. We used the most up-to-date global hydrological models, in particular the latest version of the Water Gap Hydrological Model [26] that models natural variability in addition to human intervention.

2.2.4. Land Ice Component

Land ice melt associated with current global warming is an important contribution to the GRACE fields. Global glaciers are currently melting [27], and the ice sheets (Greenland and Antarctica) are losing mass at an accelerated rate, e.g., [28] and also the IMBIE 2 project (<http://www.climate-cryosphere.org/media-gallery/1626-shepherd>). Three main methods are used to estimate the mass

balance of the ice sheets: (1) measurement of changes in elevation of the ice surface over time from radar altimetry; (2) the mass budget or input–output method, which involves estimating the difference between the surface mass balance and ice discharge; and (3) the redistribution of mass using GRACE. For the glaciers, GRACE is also used, but the main methodologies to estimate mass change are in situ measurements combined with models. For both the glaciers and ice sheets, we used estimates based on non-GRACE approaches as described in detail by the World Climate Research Program (WCRP) Global Sea Level Budget Group [29].

2.2.5. Ocean Mass Change

The dominant signal for ocean mass change is the one due to the present day land ice melt. It is routinely measured by GRACE, e.g., [29]. The best alternative to obtain independent data is the use of gridded sea level fields from satellite altimetry corrected for ocean thermal expansion. Six different altimetry datasets are available, including the most recently improved one in the context of the ESA Climate Change Initiative project [30]. Several ocean thermal expansion datasets are also available from expendable bathythermograph (XBT) and Argo (international program) profiling float measurements (temperature, salinity, currents, and bio-optical properties) [31]. These datasets (altimetry and thermal expansion) are described in detail in [29].

2.2.6. GIA and Other Static Factors

GIA induces important regional trends in GRACE solutions (e.g., [11,12]). To correct GRACE data for the GIA, global models are used. These models depend on the deglaciation history and mantle viscosity profile. In Reference [19], three different solutions are considered to estimate model discrepancies and their impact on GRACE solutions. The ensemble mean GRACE solution considered here is corrected for the ICE6G-C GIA model [32].

2.2.7. Remaining Effects—Core Effects

The gridded GRACE-based gravity time series were corrected for all effects described above (land water storage, land ice, and GIA). We refer to the residual gravity field as the corrected GRACE-based gridded time series. We applied empirical orthogonal function (EOF) analysis decomposition [33] to the residual GRACE gravity field to investigate the signal and its spatiotemporal variability that remains after applying all above corrections. This approach can be used to identify the different modes of spatial and temporal variability of a signal. The first modes are associated with the largest variance of the total signal and in principle represent their dominant spatiotemporal components. The dominant inter-annual gravity signal (first EOF mode) is the one that correlates with the residual magnetic signal.

The gravity residuals include the signature of processes occurring in the core and at the core–mantle boundary (CMB). In addition to the topography generated by the convection in the mantle, e.g., [34], the CMB may be in a dynamic equilibrium state, mainly controlled by dissolution–crystallization processes, by the infiltration of the liquid core alloy in the overlying mantle silicate rocks [2], as well as a compaction process induced by the core flow on the mantle [34,35].

3. Results

In a pioneering article, Reference [1] reported the existence of a correlation between spatiotemporal variations of the magnetic and gravity fields at an inter-annual timescale. This correlation was later interpreted as reflecting processes occurring at the CMB [2]. The measured anomalies of a few tens nT/y^2 in the core magnetic field secular acceleration and of hundreds of nGal in the gravity field, obtained from the highest-sensitivity satellite measurements, are compatible with the estimated effect of the dissolution–infiltration process.

We revisited the results published by [1], mainly to investigate how the two fields correlate over a longer period of time. In Reference [1], the considered time span starts in August 2002 and ends in August 2010. Here, the considered period is from January 2003 to December 2015. In addition,

the models used for the corrections of the observed fields are different from the previous study. For the magnetic field, we used the series of field variations as provided by the CHAOS-6 model (<http://www.spacecenter.dk/files/magnetic-models/CHAOS-6/>), providing the most precise values of the secular acceleration of the vertical magnetic field component. For the gravity field, the series were obtained from the pre-processed LEGOS V0.94 mean value model (ftp.legos.obs-mip.fr/pub/soa/gravimetry/grace_legos). Note that for the few missing months, a cubic spline was applied with respect of the annual and semi-annual cycles and the trend, and to minimize the sub-annual signals, a Hamming window of 15 months was applied. Over the indicated period, both models were truncated at degree/order 8 in order to characterize the large spatial scale. These two models were considered for reconstructing the corresponding magnetic and gravity time series on a global grid defined by 10° in geographic latitude and 20° in geographic longitude; this can be considered to be a well-distributed network of “virtual magnetic and gravity observatories” (VMGOs) located at the center of each cell. At the position of each observatory, series of both fields were computed as monthly means.

Considering that the core processes are large-scale phenomena, the common variability of the magnetic and gravity fields was investigated at a global scale. We chose to apply, as in [1], the singular value decomposition (SVD) technique, which is generally used to retrieve common variability modes from two datasets [36]. This can be seen as a generalization of the empirical orthogonal function decomposition, which isolates common variability modes in a set of time series. Applying this method allowed us to retrieve this common variability for all the VMGOs by decomposing the two sets of time series into a number of modes of common variation. Each mode consists of a spatial pattern and a time series for each dataset. The temporal variations are smoothed with a 6-month window. Figure 2 shows temporal and spatial variations of the parts of the gravity and magnetic fields interpreted as originating in the core after minimizing the contributions from surface and external sources and subtracting the annual signal and the mean. It is possible to detect large-scale magnetic and mass distribution fluctuations. The associated time series show a slow oscillation at the sub-decadal timescale, consistent with the suddenness of geomagnetic jerks [37], as was the case in the events detected in 2007.5 [38] and 2014.5 [39].

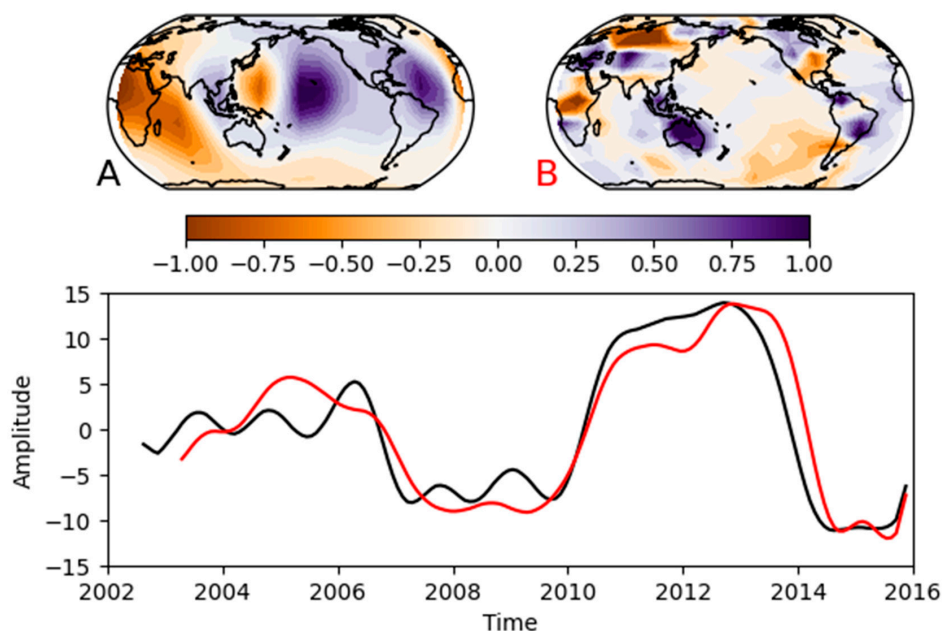


Figure 2. Results of the singular value decomposition (SVD) applied to gravity and magnetic series. The upper panel shows the spatial pattern of the decomposition dominant mode for the gravity field (A) and for the magnetic field (B). The bottom panel shows the temporal behavior of the two series: amplitudes of the secular acceleration of the vertical downward geomagnetic field component (red, in nT/yr²) and of the gravity field (black, in mm equivalent water height/EHW).

This study, together with those by [1,2], suggests that the core flows produce a signature in both magnetic and gravity variations at a decadal timescale. The physical mechanisms causing the reported common variability result in different geographical patterns at different times in magnetic and in gravity signals. The applied analysis allowed us to retrieve the dominant time structure of the variability for each field.

Additional computations are required in order to further investigate these correlations. As there is no reason why the magnetic and gravity signatures should be localized at the same position on Earth, these signatures could be unsynchronized. Some methods have been proposed to study unsynchronized correlations and causalities, such as singular spectrum analysis, see [40] and references therein, and they can be applied for such investigations. The structure of the common time variability is also worth investigating, as it can bring insight into the physical process. Investigating the newly available magnetic and gravity data and developing new techniques in signal separation might allow a better localization of the phenomena, resulting in a better description of the common variability.

4. Discussion

The promising results on this topic led the authors to develop the GRACEFUL project, recently selected by the ERC in the context of its SYNERGY program. The project aims at building on the well-known correlation between the magnetic field and LoD variations in addition to the abovementioned correlation between magnetic and gravity fields. We will refine the latter correlation by improving the GRACE data analysis using all available datasets for correcting the near surface signals and estimating associated uncertainties. We will also use the most up-to-date LoD data at a decadal timescale to infer the flow patterns inside the core. The core flow generated by the Earth's rotation itself will be studied in conjunction with the flow induced by the magnetic field. The effect of the CMB topography and the interactions between the core and the mantle at the CMB and of an inner core will be taken into account to quantify induced gravity changes. Furthermore, we will use the recent core modelling tools developed in the frame of the Rotation and Nutation of a wobbly Earth (RotaNut) ERC to infer the core flows that explain all these observations. The project aims to critically improve our understanding of the liquid core dynamics from cutting-edge LOD, magnetic field, and gravity observations, as well as most comprehensive flow models capitalizing on the models and expertise developed in the frame of the ERC Advanced Grant RotaNut led in recent years by a member of our team.

Author Contributions: Conceptualization, M.M., V.D., A.C.; investigation, M.M., V.D., A.C.; writing—review and editing, M.M., V.D., A.C. All authors have read and agreed to the published version of the manuscript.

Funding: The research leading to these results has received funding from the European Research Council (ERC) Advanced Grant No 670874, RotaNut—Rotation and Nutation of a wobbly Earth, as well as from the ERC GRACEFUL Synergy Grant No 855677.

Acknowledgments: We would like to thank Olivier de Viron for discussions and inputs in data analysis, Alejandro Blazquez for the GRACE data analysis, and Ingo Wardinski for magnetic data analysis. We also thank the three referees for very constructive suggestions to improve the manuscript.

Conflicts of Interest: The authors declare no conflict of interest.

References

1. Mandea, M.; Panet, I.; Lesur, V.; De Viron, O.; Diament, M.; Le Mouél, J.-L. Recent changes of the Earth's core derived from satellite observations of magnetic and gravity fields. *Proc. Natl. Acad. Sci. USA* **2012**, *109*, 19129–19133. [[CrossRef](#)] [[PubMed](#)]
2. Mandea, M.; Narteau, C.; Panet, I.; Le Mouél, J.-L. Gravimetric and magnetic anomalies produced by dissolution-crystallization at the core-mantle boundary. *J. Geophys. Res. Solid Earth* **2015**, *120*, 5983–6000. [[CrossRef](#)]
3. Cox, C.; Chao, B.F. Detection of large-scale mass redistribution in the terrestrial system since 1998. *Science* **2002**, *297*, 831–833. [[CrossRef](#)] [[PubMed](#)]

4. Cheng, M.; Ries, J.C.; Tapley, B.D. Variations of the Earth's figure axis from satellite laser ranging and GRACE. *J. Geophys. Res.* **2011**, *116*, B01409. [[CrossRef](#)]
5. Meyssignac, B.; Lemoine, J.M.; Cheng, M.; Cazenave, A.; Gegout, P.; Maisongrande, P. Interannual variations in degree-two Earth's gravity coefficients C_{2,0}, C_{2,2} and S_{2,2} reveal large-scale mass transfers of climatic origin. *Geophys. Res. Lett.* **2013**, *40*, 1–6. [[CrossRef](#)]
6. Wahr, J.M. Time-Variable Gravity from Satellites. *Treatise Geophys.* **2015**, *3*, 193–213. [[CrossRef](#)]
7. Tapley, B.; Watkins, M.; Flechtner, F.; Reigber, C.; Bettadpur, S.; Rodell, M.; Sasgen, I.; Famiglietti, J.S.; Landerer, F.W.; Chambers, D.P.; et al. Contributions of GRACE to understanding climate change. *Nat. Clim. Chang.* **2019**, *5*, 358–369. [[CrossRef](#)]
8. Cazenave, A.; Souriau, A.; Dominh, K. Global coupling of Earth surface topography with hotspots, geoid and mantle heterogeneities. *Nature* **1989**, *340*, 54–57. [[CrossRef](#)]
9. Panet, I.; Mikhailov, V.; Diament, M.; Pollitz, F.; King, G.; de Viron, O.; Holschneider, M.; Biancale, R.; Lemoine, J.-M. Coseismic and post-seismic signatures of the Sumatra 2004 December and 2005 March earthquakes in GRACE satellite gravity. *Geophys. J. Int.* **2007**, *171*, 177–190. [[CrossRef](#)]
10. de Viron, O.; Panet, I.; Mikhailov, V.; Van Camp, M.; Diament, M. Retrieving earthquake signature in GRACE gravity solutions. *Geophys. J. Int.* **2008**, *174*, 14–20. [[CrossRef](#)]
11. Peltier, W.R. Global glacial isostasy and the surface of the ice-age Earth: The ICE-5G (VM2) model and GRACE. *Annu. Rev. Earth Planet. Sci.* **2004**, *32*, 111–149. [[CrossRef](#)]
12. Tamisiea, M.E. Ongoing glacial isostatic contributions to observations of sea level change. *Geophys. J. Int.* **2011**, *186*, 1036–1044. [[CrossRef](#)]
13. Adhikari, S.; Ivins, E.R.; Frederikse, T.; Landerer, F.W.; Caron, L. Sea level fingerprints emergent from GRACE mission data. *ESSD* **2019**, *11*, 629–646. [[CrossRef](#)]
14. Lesur, V.; Rother, M.; Vervelidou, F.; Hamoudi, M.; Thébault, E. Post-processing scheme for modeling the lithospheric magnetic field. *Solid Earth Discuss.* **2012**, *4*, 1345–1378. [[CrossRef](#)]
15. Finlay, C.C.; Olsen, N.; Kotsiaros, S.; Gillet, N.; Toffner-Clausen, L. Recent geomagnetic secular variation from Swarm and ground observatories as estimated in the CHAOS-6 geomagnetic field model. *Earth Planets Space* **2016**, *68*. [[CrossRef](#)]
16. Wardinski, I.; Holme, R. Signal from noise in geomagnetic field modelling: Denoising data for secular variation studies. *Geophys. J. Int.* **2011**, *185*, 653–662. [[CrossRef](#)]
17. Cox, G.A.; Brown, W.J.; Billingham, L.; Holme, R. MagPySV: A Python package for processing and denoising geomagnetic observatory data. *Geochem. Geophys. Geosyst.* **2018**, *19*. [[CrossRef](#)]
18. Stammer, D.; Cazenave, A.; Ponte, R.; Tamisiea, M. Contemporary regional sea level changes. *Annu. Rev. Mar. Sci.* **2013**, *5*, 21–46. [[CrossRef](#)]
19. Blazquez, A.; Meyssignac, B.; Lemoine, J.M.; Berthier, E.; Ribes, A.; Cazenave, A. Exploring the uncertainty in GRACE estimates of the mass redistributions at the Earth surface: Implications for the global water and sea level budgets. *Geophys. J. Int.* **2018**, *215*, 415–430. [[CrossRef](#)]
20. Swenson, S.; Chambers, D.; Wahr, J. Estimating geocenter variations from a combination of GRACE and ocean model output. *J. Geophys. Res.* **2008**, *113*. [[CrossRef](#)]
21. Cheng, M.; Tapley, B.D.; Ries, J.C. Deceleration in the Earth's oblateness. *J. Geophys. Res.* **2013**, *118*, 740–747. [[CrossRef](#)]
22. Geruo, A.; Wahr, J.; Zhong, S. Computations of the viscoelastic response of a 3-D compressible Earth to surface loading: An application to Glacial Isostatic Adjustment in Antarctica and Canada. *Geophys. J. Int.* **2013**, *192*, 557–572.
23. Cazenave, A.; Dieng, H.; Meyssignac, B.; von Schuckmann, K.; Decharme, B.; Berthier, E. The rate of sea level rise. *Nat. Clim. Chang.* **2014**, *2014*, 358–361. [[CrossRef](#)]
24. Reager, J.T.; Gardner, A.S.; Famiglietti, J.S.; Wiese, D.N.; Eicker, A.; Lo, M.H. A decade of sea level rise slowed by climate-driven hydrology. *Science* **2016**, *351*, 699–703. [[CrossRef](#)]
25. Scanlon, B.; Zhang, R.; Save, Z.; Sun, H.; Schmied, A.Y.; van Beek, H.M.; Longuevergne, L. Global models underestimate large decadal declining and rising water storage trends relative to GRACE satellite data. *Proc. Natl. Acad. Sci. USA* **2018**, *115*, E1080–E1089. [[CrossRef](#)]
26. Doell, P.; Douville, H.; Güntner, A.; Müller Schmied, H.; Wada, Y. Modelling freshwater resources at the global scale: Challenges and prospects. *Surv. Geophys.* **2017**, *37*, 195–221. [[CrossRef](#)]

27. Marzeion, B.; Champollion, N.; Haeberli, W.; Langley, K.; Leclercq, P.; Paul, F. Observation-Based Estimates of Global Glacier Mass Change and Its Contribution to Sea-Level Change. *Surv. Geophys.* **2017**, *28*, 105–130. [[CrossRef](#)]
28. Bamber, J.L.; Westaway, R.M.; Marzeion, B.; Wouters, B. The land ice contribution to sea level during the satellite era. *Environ. Res. Lett.* **2018**, *13*, 063008. [[CrossRef](#)]
29. WCRP Global Sea Level Budget Group. Global sea level budget, 1993-present. *Earth Syst. Sci. Data* **2018**, *10*, 1551–1590. [[CrossRef](#)]
30. Legeais, J.F.; Ablain, M.; Zawadzki, L.; Zuo, H.; Johannessen, J.A.; Scharffenberg, M.G.; Fenoglio-Marc, L.; Fernandes, J.; Andersen, O.B.; Rudenko, S.; et al. An improved and homogeneous altimeter sea level record from the ESA Climate Change Initiative. *Earth Syst. Sci. Data* **2018**, *10*, 281–301. [[CrossRef](#)]
31. Von Schuckman, K.; Le Traon, P.-Y.; Smith, N.; Pascual, A.; Djavidnia, S.; Gattuso, J.-P.; Marilaure, G.; Nolan, G.; Aaboe, S.; Aguiar, E.; et al. Copernicus Marine Service Ocean State Report, Issue 3. *J. Oper. Oceanogr.* **2019**, *12* (Suppl. S1), 1–123. [[CrossRef](#)]
32. Stuhne, G.R.; Peltier, W.R. Reconciling the ICE-6G C reconstruction of glacial chronology with ice sheet dynamics: The cases of Greenland and Antarctica. *J. Geophys. Res.* **2015**, *120*, 1841–1865. [[CrossRef](#)]
33. Preisendorfer, R.W. Principal Component Analysis in Meteorology and Oceanography. *Dev. Atmos. Sci.* **1988**, *17*, XVIII-425.
34. Dehant, V.; Wahr, J.M. The response of a compressible, non-homogeneous Earth to internal loading: Theory. *J. Geomagn. Geoelectr.* **1991**, *43*, 157–178. [[CrossRef](#)]
35. Poirier, J.P.; Le Mouél, J.-L. Does infiltration of core material into the lower mantle affect the observed geomagnetic field? *Phys. Earth Planet. Inter.* **1992**, *73*, 29–37. [[CrossRef](#)]
36. Storch, H.; Zwiers, F. *Statistical Analysis in Climate Research*; Cambridge University Press: Cambridge, UK, 1999. [[CrossRef](#)]
37. Manda, M.; Holme, R.; Pais, A.; Pinheiro, K.; Jackson, A.; Verbanac, G. Geomagnetic Jerks: Rapid Core Field Variations and Core Dynamics. *Space Sci. Rev.* **2010**, *155*, 147–175. [[CrossRef](#)]
38. Olsen, N.; Manda, M.; Sabaka, T.J.; Tøffner-Clausen, L. CHAOS-2—A geomagnetic field model derived from one decade of continuous satellite data. *Geophys. J. Int.* **2009**, *179*, 1477–1487. [[CrossRef](#)]
39. Torta, J.M.; Pavon-Carrasco, F.J.; Marsal, S.; Finlay, C.C. Evidence for a new geomagnetic jerk in 2014. *Geophys. Res. Lett.* **2015**, *42*, 7933–7940. [[CrossRef](#)]
40. Ghil, M.; Allen, R.M.; Dettinger, M.D.; Ide, K.; Kondrashov, D.; Mann, M.E.; Robertson, A.W.; Saunders, A.; Tian, Y.; Varadi, F. Advanced spectral methods for climatic time series. *Rev. Geophys.* **2002**, *40*, 3.1–3.41. [[CrossRef](#)]

Publisher’s Note: MDPI stays neutral with regard to jurisdictional claims in published maps and institutional affiliations.



© 2020 by the authors. Licensee MDPI, Basel, Switzerland. This article is an open access article distributed under the terms and conditions of the Creative Commons Attribution (CC BY) license (<http://creativecommons.org/licenses/by/4.0/>).